Simulation of Steady State Laser Hardening

H.J.M. Geijselaers, Yuhong Yu* and J.Huétink
Mechanical Engineering, University of Twente,
* Netherlands Institute of Metals Research,
Po Box 217, 7500 AE Enschede, The Netherlands

ABSTRACT: A method for one step analysis of steady state processes, which is called the "displacement based reference frame" formulation, has been presented in (Balagangadhar and Tortorelli 1998) and has been applied to thermal processing in (Balagangadhar et al. 1999) and (Ruan 1999). In this paper we develop a similar method. Only the primary variables displacements ($\mathbf{u}$) and heat flows ($\mathbf{q}$) are used as nodal variables. For integration of material derivatives of secondary variables plastic strain, temperature and phase fraction the Discontinuous Galerkin method is used. We apply the method to the simulation of laser hardening of a steel slab.

1 INTRODUCTION

With help of a laser beam the surface of a workpiece can be locally heated at very high rates. After the beam has passed, the high thermal gradients induce a very high cooling rate by conduction to the cold bulk. Proper choice of the scanning velocity and power density causes a thermal cycle where eventually the treated surface fully transforms to martensite, a hard and wear resistant phase.

The main points of interest when doing simulations are the thickness of the hardened layer, the residual stresses and the eventual distortion of the workpiece.

When a window is defined fixed to the laser beam and the material is made to pass through the window, hardening with a scanning laser beam can be viewed as a steady state process.

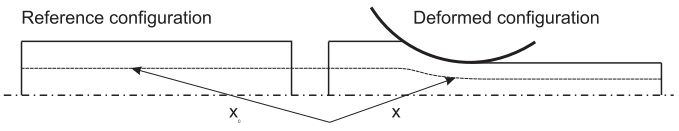

Figure 1: Rolling as an example of a steady state process.

Consider as an example of a steady state process, rolling as shown in figure 1. The usual way to analyze this process would be to prescribe the velocities or displacement increments in the roll-workpiece contact area. An analysis carried out this way would give as result a velocity field, from which through streamline integration stresses and free surface locations have to be calculated. This method has been called the "Rate equilibrium formulation" in (Thompson and Yu 1990).

An alternative way of analyzing arises when we compare an identical slab of workpiece material at two different instances. The reference configuration is when this slab has not yet entered the work zone of the process. The deformed configuration is when the volume under consideration has, at some time later, entered the work zone and is being processed.

Comparison of the locations of "identical" material points in both configurations will directly yield the deformation gradient.
Suitable differentiation of the deformation gradient along the streamline will yield a deformation rate.
This deformation rate is then used to calculate a plastic deformation rate. Integration of the plastic deformation rate along the streamline yields the plastic deformations. The elastic strains are found after subtracting the plastic deformations from the actual deformations. Then the stresses are known. These stresses are used to check whether the deformed configuration is indeed in equilibrium.
When this is not the case, the locations of the material points are updated and the calculation is reiterated.

In (Balagangadhar et al. 1999) the plastic strains are nodal variables also and enter in the system matrix. In our implementation we will show that only displacements and heat flows are needed

As is apparent from figure 1 locating the streamlines in the reference configuration is a trivial task. It is obvious that all streamline integration as well as differentiations along streamlines will be done in this configuration.

2 GOVERNING EQUATIONS

2.1 Phase Transformations

Two types of phase transformations are discerned, diffusion related transformations and martensite transformations. The evolution of diffusion related transformations is described by an S-curve, the Avrami equation.

$$\varphi(t) = \varphi_0 + (\bar{\varphi} - \varphi_0)(1 - \mathrm{e}^{-(t/\tau)^n}) \tag{1}$$

Here φ_0 is the initial fraction, while $\bar{\varphi}(T)$ is the amount of phase that should be present according to the equilibrium phase diagram, $n(T)$ and $\tau(T)$ are material parameters derived from TTT (time-temperature-transformation) diagrams. The martensite transformation is described by the Koistinen-Marburger relation.

$$\varphi(T) = \varphi_{\gamma Ms}(1 - \mathrm{e}^{-\beta(T - T_{Ms})}) \tag{2}$$

Here $\varphi_{\gamma Ms}$ is the amount of austenite which is still present at the martensite start temperature T_{Ms}. Both equations are used in a rate form, where the eventual phase contents is found by integration along the streamlines.

$$\mathbf{v} \cdot \nabla\varphi = \dot{\varphi} \tag{3}$$

2.2 Mechanical Equilibrium

The mechanical equilibrium equation in the absence of body forces is:

$$\boldsymbol{\sigma} \cdot \nabla = \mathbf{0} \tag{4}$$

For the constitutive equations a parallel fraction model is used (Geijselaers and Huétink 1995). The Cauchy stress is a weighted sum of the stresses in the different phases.

$$\boldsymbol{\sigma} = \sum_i \varphi^i \boldsymbol{\sigma}^i \tag{5}$$

Here φ^i is the fraction of the i^{th} phase. The strain is the summation of an elastic strain, a plastic strain and contributions from transformation strain, thermal dilatation and transformation plasticity. Small strain is assumed to be sufficiently accurate.

$$\begin{aligned} \boldsymbol{\varepsilon} &= \boldsymbol{\varepsilon}^{el(i)} + \boldsymbol{\varepsilon}^{pl(i)} + \boldsymbol{\varepsilon}^{tr} + \boldsymbol{\varepsilon}^{th} + \boldsymbol{\varepsilon}^{tp(i)} \\ \boldsymbol{\varepsilon} &= \frac{1}{2}(\mathbf{u}\nabla + \nabla\mathbf{u}) \end{aligned} \tag{6}$$

formation strain is:

$$\begin{aligned} &\boldsymbol{\varepsilon}^{tr} + \boldsymbol{\varepsilon}^{th} = ((\rho_0/\rho)^{1/3} - 1)\mathbf{I} \\ &\text{where:} \quad \rho(\varphi, T) = \sum_i \varphi^i \rho^i \end{aligned} \tag{7}$$

Here $\rho_i(T)$ is the density of phase i. The transformation plasticity is linked to the deviatoric stress $\mathbf{s}$ in the phase. This is governed by a rate equation.

$$\mathbf{d}^{tp(i)} = \tfrac{3}{2} K^i \dot{\varphi}^i \mathbf{s}^i \tag{8}$$

the constants K^i depend on the chemical composition of the steel and on the type of transformation. The values of K^i must be obtained from tests.

The description of plastic deformation is based on the Von Mises yield criterion with isotropic hardening. Plastic deformation of a phase occurs, when the deviatoric stress in this phase exceeds the yield surface.

$$\Phi^i(\mathbf{s}^i, \varepsilon^{p(i)}, T) = \mathbf{s}^i : \mathbf{s}^i - \tfrac{2}{3}(\sigma_y^i(\varepsilon^{p(i)}, T))^2 = 0 \tag{9}$$

Here ε^p is the equivalent plastic strain. Using classical flow theory for plasticity, we find an expression for the plastic strain rate.

$$\begin{aligned} \mathbf{d}^{pl(i)} = \frac{3}{3G^i + \frac{\partial\sigma_y^i}{\partial\varepsilon^{p(i)}}} \{ &\frac{3G^i}{2} \frac{\mathbf{s}^i \mathbf{s}^i}{(\sigma_y^i)^2} : \mathbf{d} - \\ &\frac{3G^i}{2} K^i \mathbf{s}^i \dot{\varphi}^i + \frac{\mathbf{s}^i}{2G^i \sigma_y^i} (\frac{\mathrm{d}G^i}{\mathrm{d}T} \sigma_y^i - G^i \frac{\partial\sigma_y^i}{\partial T}) \dot{T} \} \end{aligned} \tag{10}$$

The plastic strain rate and the transformation plasticity rate per fraction are integrated along the streamlines to obtain the plastic strain.

$$\mathbf{v} \cdot \nabla(\boldsymbol{\varepsilon}^{pl(i)} + \boldsymbol{\varepsilon}^{tp(i)}) = \mathbf{d}^{pl(i)} + \mathbf{d}^{tp(i)} \tag{11}$$

This is a scalar equation, which applies to every component of the tensors. We call it the convection equation. After integration of the plastic strain rates to plastic strains, the fraction stress is calculated.

$$\begin{aligned} \boldsymbol{\sigma}^i &= \mathbf{E}^i : (\boldsymbol{\varepsilon} - \boldsymbol{\varepsilon}^{pl(i)} - \boldsymbol{\varepsilon}^{tp(i)} - \boldsymbol{\varepsilon}^{th} - \boldsymbol{\varepsilon}^{tr}) \\ &= \mathbf{E}^i : \boldsymbol{\varepsilon} - 2G^i(\boldsymbol{\varepsilon}^{pl(i)} + \boldsymbol{\varepsilon}^{tp(i)}) \\ &\quad - \frac{2G^i(1+\nu^i)}{1-2\nu^i}(\varepsilon^{th} + \varepsilon^{tr})\mathbf{I} \end{aligned} \tag{12}$$

2.3 Thermal Equilibrium

The equation of conservation of energy is:

$$\nabla \cdot (k\nabla T) - \rho\dot{e} = 0 \tag{13}$$

Here k is the conductivity coefficient. ρ Is the mass density and e is the specific internal energy. The

phase.

$$\rho e = \sum_i \rho^i \varphi^i e^i = \rho \sum_i \frac{\rho^i}{\rho} \varphi^i e^i \tag{14}$$

Per fraction the internal energy is a function of the temperature, obtained by integration of the specific heat c_p.

$$e^i(T) = \int_{T_0}^{T} c_p^i(T) \mathrm{d}T + e_0^i \tag{15}$$

An approximate expression for the rate of the internal energy is then found.

$$\rho \dot{e} = \sum_i \rho^i \varphi^i c_p^i \dot{T} + \sum_i \rho^i e^i \dot{\varphi}^i \tag{16}$$

The first term is the regular specific heat, the second term is a model of latent heat of phase transformation. The resulting rate equation of thermal equilibrium is:

$$\sum_i \rho^i \varphi^i c_p^i \dot{T} = -\sum_i \rho^i e^i \dot{\varphi}^i + \nabla \cdot (k \nabla T) \tag{17}$$

To obtain the temperatures the temperature rate has to be integrated. For a steady state process the time integration is again replaced by an integration along the streamlines.

$$\mathbf{v} \cdot \nabla T = \dot{T} \tag{18}$$

3 DISCRETIZATION

3.1 Convection equation

The streamline integration of any quantity f, be it a strain component, phase fraction, equivalent plastic strain or temperature, is described by the convection equation.

$$\mathbf{v} \cdot \nabla f = \dot{f} \tag{19}$$

Using the deformation gradient $\mathbf{F}$ this can be transformed to the undeformed configuration.

$$\begin{aligned} \mathbf{v} \cdot \nabla f =& \mathbf{v} \cdot \mathbf{F}^{\mathrm{T}} \cdot \mathbf{F}^{-\mathrm{T}} \cdot \nabla f = \\ =& \mathbf{v}_0 \cdot \nabla_0 f = v_0 \frac{\partial f}{\partial x_0} \end{aligned} \tag{20}$$

A very stable discretization of the convection equations (11) and (18) is the Discontinuous Galerkin method (Fortin and Fortin 1989).

$$\begin{aligned} v_0 \int_{V_0} \bar{f} \frac{\partial f}{\partial x} \mathrm{d}V - v_0 \int_{\Gamma_{in0}} n_x \bar{f} (f - f^{upw}) \mathrm{d}A = \\ = \int_{V_0} \bar{f} \dot{f} \mathrm{d}V \end{aligned} \tag{21}$$

the jump at the inflow boundary of every element is weighted. Since the convection equation is a first order equation, only the boundary condition at the inflow of the element is taken into account, the jump at the outflow is disregarded. In this way the necessary upwinding is realized.

To obtain a well posed problem the initial condition at the inflow of the domain has to be taken into account also. The solutions obtained this way for the convection equations are free of spurious oscillations and show hardly any cross wind diffusion. The resulting matrix equations will have a form like:

$$[\mathrm{D}]\{\mathrm{f}^e\} = [\mathrm{B}]\{\dot{\mathrm{f}}^e\} + \{\mathrm{f}_0\} \tag{22}$$

All quantities which are defined inside the elements and which are interpolated by discontinuous functions are written with the suffix $()^e$. Effectively these are variables, which are defined in the integration points.

3.2 Thermal equations

The temperature field which results from the convection equation is discontinuous across element boundaries. Therefore a discretization of the thermal conduction equation is used, which can cope with discontinuous temperatures. The primary variables are the heat fluxes $\mathbf{q}$ in the nodes. The temperatures are treated as dependent element variables. Equation (17) is partitioned into a heat flow equation and a temperature rate equation.

$$\begin{aligned} \mathbf{q} &= -k \nabla T \\ \sum_i \rho^i \varphi^i c_p^i \dot{T} &= -\nabla \cdot \mathbf{q} - \sum_i \rho^i e^i \dot{\varphi}^i \end{aligned} \tag{23}$$

The temperatures are discontinuous across element boundaries. The T-interpolation in each element is independent from the neighbors. This means that the second equation can be solved to find the temperature rates directly in the integration points. Only the first equation needs to be discretized. The temperature jumps across the element boundaries are also weighted.

$$\begin{aligned} \int_V \bar{\mathbf{q}} \cdot \mathbf{q} \mathrm{d}V = -\int_V k \bar{\mathbf{q}} \cdot \nabla T \mathrm{d}V + \\ + \sum_{i=1}^{N_{el}} \int_{\Gamma_i} k \bar{\mathbf{q}} \cdot \mathbf{n} (T - T_0) \mathrm{d}A \end{aligned} \tag{24}$$

After applying partial integration the inter-element integrals cancel out and we find

$$\int_V \bar{\mathbf{q}} \cdot \mathbf{q} \mathrm{d}V = \int_V k (\nabla \cdot \bar{\mathbf{q}}) T \mathrm{d}V - \int_\Gamma k \bar{\mathbf{q}} \cdot \mathbf{n} T_0 \mathrm{d}A \tag{25}$$

temperatures need to match. A quadratic **q**-field matches with a linear T-interpolation.
In the specification of the boundary conditions the role of the temperatures and heat flows are reversed when compared to conventional thermal modeling. The heat flow is now a kinematical boundary condition, the temperature is a natural boundary condition. When no boundary condition is specified, the temperature is zero.

The resulting matrix equations are written as

$$\begin{aligned} [\mathrm{M}]\{\mathrm{q}\} &= [\mathrm{C}]\{\mathrm{T}^e\} + \{\mathrm{Q}\} \\ \{\dot{\mathrm{T}}^e\} &= [\mathrm{L}]\{\mathrm{q}\} + \{\dot{\Phi}_T\} \\ [\mathrm{D}]\{\mathrm{T}^e\} &= [\mathrm{B}]\{\dot{\mathrm{T}}^e\} + \{\mathrm{T}_0\} \end{aligned} \tag{26}$$

3.3 Mechanical Equilibrium

The mechanical equilibrium equation (4) is written in a weak form using a vector weight function $\bar{\mathbf{u}}$. Since the stresses are discontinuous across element boundaries, the jumps have to be weighted.

$$\int\limits_V \bar{\mathbf{u}} \cdot \boldsymbol{\sigma} \cdot \nabla \mathrm{d}V - \sum_{i=1}^{N_{el}} \int\limits_{\Gamma_i} \bar{\mathbf{u}} \cdot (\boldsymbol{\sigma} \cdot \mathbf{n} - \mathbf{t}_0) \mathrm{d}A = \mathbf{0} \tag{27}$$

After partial integration the inter-element boundary terms cancel out. Only terms dealing with the prescribed stress boundaries Γ_σ remain.

$$\int\limits_V (\bar{\mathbf{u}}\nabla) : \boldsymbol{\sigma} \mathrm{d}V = \int\limits_{\Gamma_\sigma} \bar{\mathbf{u}} \cdot \mathbf{t}_0 \mathrm{d}A \tag{28}$$

The plastic strain rates in the elements are calculated using equations (8) and (10). The strain rates are integrated to strains using equation (11). This results in a system of matrix equations.

$$\begin{aligned} [\mathrm{K}]\{\mathrm{u}\} &= [\mathrm{W}]\{\varepsilon^{pl(e)}\} + \{\mathrm{F}(T,\varphi)\} \\ \{\mathrm{d}^{pl(e)}\} &= [\mathrm{Y}]\{\mathrm{u}\} + [\mathrm{G}]\{\dot{T}^e\} + \{\dot{\Phi}_d\} \\ [\mathrm{D}]\{\varepsilon^{pl(e)}\} &= [\mathrm{B}]\{\mathrm{d}^{pl(e)}\} + \{\varepsilon_0\} \end{aligned} \tag{29}$$

The matrix [K] is the regular elastic stiffness matrix. The matrices [Y], [G] and the vector $\{\dot{\Phi}_d\}$ depend on the stress state. As a consequence this is a highly non-linear system.

3.4 The strain rate **d**

The displacement field **u** is C_0 continuous across element boundaries. This means that the strain field $\boldsymbol{\varepsilon} = \frac{1}{2}(\mathbf{u}\nabla + \nabla\mathbf{u})$ is discontinuous. The strain rate **d** is defined as the material derivative of the strain. Just taking the derivative of the discontinuous strains in the elements does not give a with neighboring elements have to be taken into account also. To do so we resort again to the discontinuous Galerkin method of section 3.1. This time it is used however in the opposite direction, to obtain material derivatives from a known discontinuous field, compare with equation (22).

$$[\mathrm{B}]\{\mathrm{d}^e\} = [\mathrm{D}]\{\varepsilon^e\} \tag{30}$$

Inspection of matrix [B] shows that it has no coupling with other elements. The only "external" coupling comes from [D], which refers to the upwind neighbors. So calculation of **d** is done element by element involving upwind neighbors only.

4 IMPLEMENTATION

Quadratic triangles are used with **u** and **q** as nodal variables. Per element three integration points are used. This implies that the interpolation of the element fields $\boldsymbol{\sigma}$, $\boldsymbol{\varepsilon}$, **d**, φ and T is linear, with the integration point values as basis.

The convection equation (19) does not change between iterations. Therefore equation (22) is solved right at the beginning. This allows for solution of the the integration point temperatures $\{\mathrm{T}^e\}$ in equations (26) in terms of the nodal point heat fluxes **q**.

$$[\mathrm{K}_{qq}]\{\mathrm{q}\} = \{\mathrm{R}_q\} \tag{31}$$

The matrices are evaluated as:

$$\begin{aligned} [\mathrm{K}_{qq}] &= [\mathrm{M}] - [\mathrm{C}][\mathrm{D}^{-1}][\mathrm{B}][\mathrm{L}] \\ \{\mathrm{R}_q\} &= \{\mathrm{Q}\} + [\mathrm{C}][\mathrm{D}^{-1}]\{\mathrm{T}_0\} + [\mathrm{C}][\mathrm{D}^{-1}][\mathrm{B}]\{\dot{\Phi}_T\} \end{aligned} \tag{32}$$

Solution requires a few iterations to account for temperature dependent properties and temperature dependent phase transformations.

Having the solution of the convection equation at hand allows us also to directly assemble a similar systems matrix for the mechanical problem.

$$[\mathrm{K}_{uu}]\{\mathrm{u}\} = \{\mathrm{R}_u\} \tag{33}$$

Symbolically the matrices can be evaluated as:

$$\begin{aligned} [\mathrm{K}_{uu}] &= [\mathrm{K}] - [\mathrm{W}][[\mathrm{D}^{-1}][\mathrm{B}][\mathrm{Y}] \\ \{\mathrm{R}_u\} &= [\mathrm{W}][[\mathrm{D}^{-1}][\mathrm{B}]([\mathrm{G}]\{\dot{\mathrm{T}}^e\} + \{\dot{\Phi}_d\}) + \\ &\quad + [\mathrm{W}][[\mathrm{D}^{-1}]\{\varepsilon_0\} + \{\mathrm{F}(T,\varphi)\} \end{aligned} \tag{34}$$

However assembly of the element matrix of one element requires looping over all elements upwind from the considered element. This implies that assembly of the system matrices of equation (34)

average size model this is prohibitive.

Our experience is that a fairly good convergence can be reached when only matrix [K] is used to find feasible solution directions. This we combine with one-dimensional line searches. In this way only the right hand side $\{R_u\}$ needs to be assembled. Convergence is slow but steady until after approximately 50 iterations the norm of the unbalance becomes lower than 1 % of $\|\{F(T,\varphi)\}\|$, the norm of the nodal forces due to thermal and transformation dilatation.

5 SIMULATIONS

We applied the presented method to a simulation of laser hardening of a steel slab. Dimensions and process parameters are shown in figure 2. The material data are chosen to represent a 0.4 % C steel (C45).

At the inflow the material consists of ferrite and pearlite, which are treated as one phase. Heated by a laser the surface quickly reaches a temperature of almost 1400 ^{0}C. The temperature distribution is shown in Figure 3.

At temperatures above A_1 (715 ^{0}C) the ferrite and pearlite transform to austenite. This transformation is modeled using an Avrami equation with temperature dependent parameters.

Due to the high thermal gradients, initially the cooling rate behind the heated zone is very high. When the temperature drops below A_1 the austenite will start transforming back to ferrite/pearlite. Also this transformation is modeled with an Avrami equation. The parameters however are such that back transformation proceeds much slower than the austenite transformation. As a result, a considerable amount of the austenite is retained.

At temperatures below M_s it will transform to martensite, the desired structure at the surface. The martensite transformation is modeled by the Koistinen-Marburger relation, which describes the equilibrium amount of martensite at the considered temperature. The martensite distribution is shown in figure 4. The martensite contents at the surface is estimated to approximately 32 %. When this is corrected for the temperature at the outflow, an amount of 45 % martensite is expected after cooling to room temperature.

The distortion of the slab is apparent from figure 2. The deformation is typical for unilaterally surface heated products. However, since this is a plain strain simulation, deformations are grossly exaggerated.

In this paper we show a one step method to obtain a solution to steady thermal processing with phase transformations. This method is based on the displacement based reference frame formulation as reported in (Balagangadhar et al. 1999). In contrast to (Balagangadhar et al. 1999) we do not have plastic strains as nodal variables. The system matrix of our mechanical problem is identical to a regular elastic stiffness matrix. This matrix is used in an iteration procedure, where only the right hand side is calculated every iteration. As a consequence more, but relatively cheap iterations are needed.

REFERENCES

Balagangadhar, D., G. Dorai, and D. Tortorelli (1999). A displacement-based reference frame formulation for steady-state thermo-elastoplastic material processes. *Int. J. Solids and Structures 36*(16?), 2397–2416.

Balagangadhar, D. and D. Tortorelli (1998). A displacement based reference frame formulation for the analysis of steady manufacturing processes. In J. Huétink and F. Baaijens (Eds.), *Simulation of Materials Processing: Theory, Methods and Applications-NUMIFORM '98*, pp. 77–83. A.A. Balkema.

Fortin, M. and A. Fortin (1989). A new approach for the fem simulation of viscoelasic flows. *Journal of Non-Newtonian Fluid Mechanics 32*, 295–310.

Geijselaers, H. and J. Huétink (1995). Finite element analysis of transformation hardening. In S. F. Shen and P. R. Dawson (Eds.), *Simulation of Materials Processing: Theory, Methods and Applications, Proceedings of the Fifth International Conference on Numerical Methods in Industrial Forming Processes-NUMIFORM '95*, pp. 259–264. A.A. Balkema.

Ruan, Y. (1999). A steady-state thermomechanical solution of continuously quenched axisymmetric bodies. *ASME Journ. Appl. Mech. 66*, 334–339.

Thompson, E. and S. Yu (1990). A flow formulation for rate equilibrium equations. *Intern. Journ. Num. Meth. Eng. 30*(8), 1619–1632.

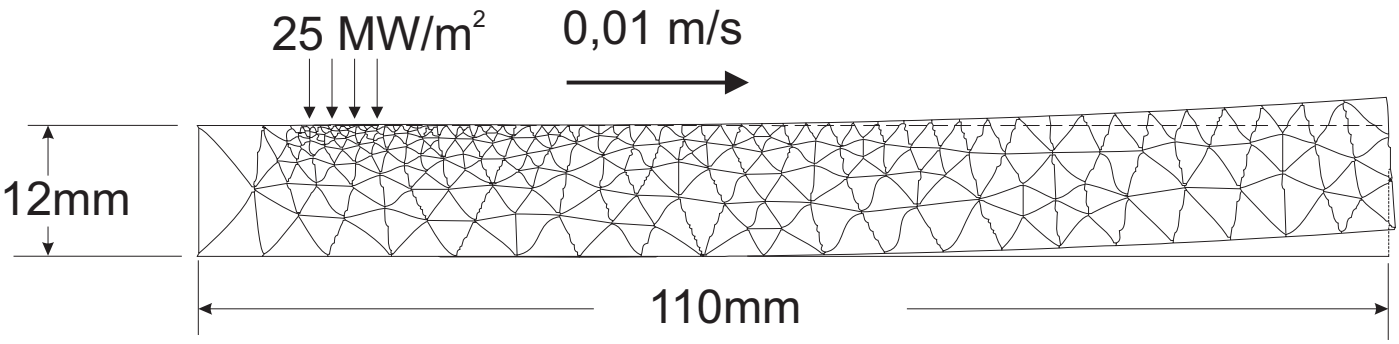

Figure 2: Laser hardening, process parameters and deformed configuration

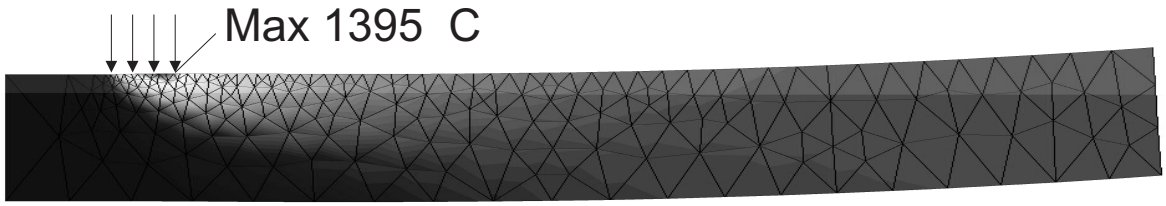

Figure 3: Temperature distribution

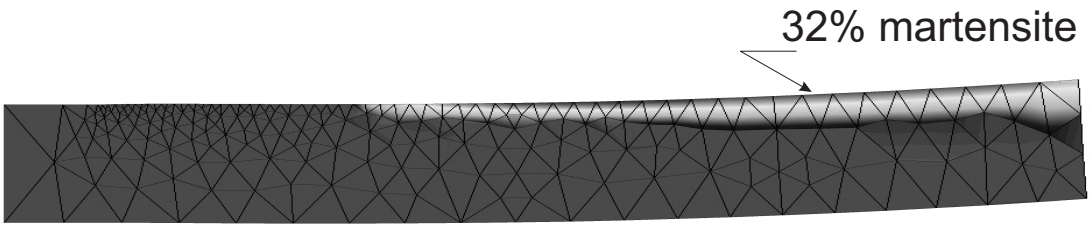

Figure 4: Martensite distribution

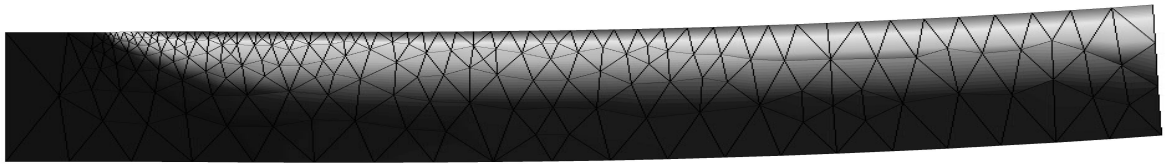

Figure 5: Distribution of the plastic strain